8) Li J, Sharma R, Patrick B, Sharma A, Jeyabal PV, Ramanjaneya V R Mula (Reddy PM), Saini MK, Dwivedi S, Dhanani S, Ansari NH, Zimniak P, Awasthi S, Awasthi YC. 2006. Regulation o...

13 AUTHORS, INCLUDING:

12253

Regulation of CD95 (Fas) Expression and Fas-Mediated Apoptotic Signaling in HLE B-3 Cells by 4-Hydroxynonenal[†]

Jie Li,[‡,§] Rajendra Sharma,[‡,§] Brad Patrick,[‡] Abha Sharma,[‡] Prince V. S. Jeyabal,[‡] Prasada M. R. V. Reddy,[‡] Manjit K. Saini,[‡] Seema Dwivedi,[‡] Shaheen Dhanani,[‡] Naseem H. Ansari,[‡] Piotr Zimniak,[‖] Sanjay Awasthi,[⊥] and Yogesh C. Awasthi*,[‡]

Department of Biochemistry and Molecular Biology, University of Texas Medical Branch, Galveston, Texas 77555, Department of Pharmacology and Department of Biochemistry and Molecular Biology, University of Arkansas for Medical Sciences and Central Arkansas Veterans Healthcare System, Little Rock, Arkansas 72205, and Department of Chemistry and Biochemistry, University of Texas, Arlington, Texas 76019

ABSTRACT: The Fas (apo/CD95) receptor which belongs to the TNF-α family is a transmembrane protein involved in the signaling for apoptosis through the extrinsic pathway. During this study, we have examined a correlation between intracellular levels of 4-HNE and expression of Fas in human lens epithelial (HLE B-3) cells. Our results show that in HLE B-3 cells, Fas is induced by 4-HNE in a concentration- and time-dependent manner, and it is accompanied by the activation of JNK, caspase 3, and the onset of apoptosis. Fas induction and activation of JNK are also observed in various tissues of *mGsta4* null mice which have elevated levels of 4-HNE. Conversely, when 4-HNE is depleted in HLE B-3 cells by a transient transfection with *hGSTA4*, Fas expression is suppressed. However, upon the cessation of *hGSTA4* expression in these transiently transfected cells, Fas and 4-HNE return to their basal levels. Fas-deficient transformed HLE B-3 cells stably transfected with *hGSTA4* show remarkable resistance to apoptosis. Also, the wild-type HLE B-3 cells in which Fas is partially depleted by siRNA acquire resistance to 4-HNE-induced apoptosis, suggesting an at least partial role of Fas in 4-HNE-induced apoptosis in HLE B-3 cells. We also demonstrate that during 4-HNE-induced apoptosis of HLE B-3 cells, Daxx is induced and it binds to Fas. Together, these results show an important role of 4-HNE in regulation of the expression and functions of Fas.

Fas antigen (apo-1/CD95) is a cell surface transmembrane glycoprotein that belongs to the tumor necrosis factor receptor (TNF-α) superfamily, which induces cell death by binding to its natural ligand (Fas L) (*1, 2*). The Fas−Fas L system is recognized as one of the major extrinsic pathways for induction of apoptosis in cells and is believed to have an essential role in maintaining homeostasis by regulating cell proliferation, differentiation, and apoptosis (*3*). Fas is expressed in many tissues; high expression levels are observed in the thymus, heart, liver, and kidney (*4*). Deficiency of Fas or Fas L in epithelial cells prevents apoptosis of these cells *in vivo* as well as *in vitro* (*5*). It has been suggested that resistance to apoptosis through the blockage of the Fas receptor might play an important role in tumorigenesis and tumor progression in several malignan-

cies (*6, 7*). In addition to its important role in the immune system, it has been suggested that the Fas−Fas L system may play an important role in the pathogenesis of diseases which are characterized by the regulation of apoptosis (*8*).

A multitude of studies during the past decade indicate a key role of 4-hydroxynonenal (4-HNE)[1] in various signaling pathways (*9−26*), including those for apoptosis. 4-HNE has been shown to modulate the expression and functions of certain key regulator membrane proteins such as tyrosine kinase receptors (*21*), PKC (*27*), and JNK (*14*). The role of 4-HNE in the regulation of Fas expression or its involvement in Fas-mediated apoptosis is not known and needs to be investigated. Our previous studies (*28, 29*) have shown that depletion of 4-HNE in human lens epithelial cells (HLE B-3) by transfection with the 4-HNE metabolizing glutathione *S*-transferase (GST) isozyme hGSTA4-4 leads to a dramatic phenotypic transformation of these cells. The transformed cells grow indefinitely in suspension as smaller, rounded cells as opposed to wild-type HLE B-3 cells which grow as attached cells with a limited life span. These transformed

* To whom correspondence should be addressed: Department of Biochemistry and Molecular Biology, 551 Basic Science Bldg., University of Texas Medical Branch, Galveston, TX 77555-0647. Telephone: (409) 772-2735. Fax: (409) 772-6603. E-mail: ycawasth@utmb.edu.
[‡] University of Texas Medical Branch.
[§] These authors contributed equally to this work.
[‖] University of Arkansas for Medical Sciences and Central Arkansas Veterans Healthcare System.
[⊥] University of Texas.

[1] Abbreviations: 4-HNE, 4-hydroxynonenal; PKC, protein kinase C; JNK, c-jun N-terminal terminal kinase; PBS, phosphate-buffered saline; TBS, Tris-buffered saline; RIPA, radioimmunoprecipitation assay buffer; PMSF, phenylmethanesulfonyl fluoride; BSA, bovine serum albumin; ROS, reactive oxygen species; PARP, poly ADP-ribose polymerase; WT, wild-type; VT, vector-transfected; Tr, *hGSTA4*-transfected.

cells lose expression of Fas, suggesting a role of 4-HNE in the regulation of Fas expression (*28, 29*). However, it could be argued that the downregulation of Fas in these cells is secondary to transformation, rather than a direct consequence of lowering of 4-HNE concentrations by transfection with *hGSTA4*. Therefore, studies are needed to examine whether 4-HNE plays a role in the regulation of the expression and functions of Fas. Furthermore, since 4-HNE has been shown to cause apoptosis in HLE B-3 and other cell lines (*30−32*), the role of Fas, if any, in 4-HNE-induced apoptosis needs to be examined. This study was designed to address these questions. We have compared the expression of Fas in HLE B-3 cells transiently or stably transfected with *hGSTA4* and examined whether a correlation exists between the intracellular levels of 4-HNE and Fas expression. The effect of exogenous 4-HNE on the expression of Fas in HLE B-3 cells has also been examined. We have previously developed a *mGsta4* null mouse model and have shown increased 4-HNE levels in the tissues of these mice (*33*). To examine whether increased 4-HNE levels in the tissues of these mice affect expression of Fas *in vivo*, we have compared Fas expression in the tissues of *mGsta4* (−/−), (+/−), and (+/+) mice. Finally, we have investigated whether Fas is involved in 4-HNE-induced apoptosis of HLE B-3 cells. The results of these studies demonstrate that the expression of Fas appears to be tightly regulated by the intracellular levels of 4-HNE and that 4-HNE-induced apoptosis in HLE B-3 cells is accompanied by the activation of Fas, JNK, and caspase 3.

MATERIALS AND METHODS

Materials. Minimum essential medium was purchased from Mediatech Inc. (Herndon, VA). Fetal calf serum was from Gemini (Woodland, CA). Phosphate-buffered saline, gentamicin, geneticin (G418), and *N*-(2-hydroxyethyl)piperazine-*N*′-2-ethanesulfonic acid (Hepes) were obtained from GIBCO Inc. (Grand Island, NY). 4-Hydroxynonenal (4-HNE) was purchased from Cayman Chemical Co. (Ann Arbor, MI). TransFast transfection reagent was from Promega (Madison, WI), and the apoptosis detection system (CaspACETM FITC-VAD-FMK *in situ* Marker) was purchased from Promega. The cytoplasmic protein extraction kit was acquired from Imgenex Co. (San Diego, CA); protein A/G−agarose beads were from Santa Cruz Biotechnology (Santa Cruz, CA), and the Western blot stripping buffer was from Pierce (Rockford, IL). All other reagents for SDS−PAGE and Western blot analysis were purchased from Bio-Rad (Hercules, CA).

Antibodies. Polyclonal antibodies against recombinant hGSTA4-4 developed in chicken were the same as those described previously (*34*). Antibodies against Fas receptor, FADD, Daxx, caspase 8, p-JNK, JNK, GAPDH, and antimouse IgG were obtained from Santa Cruz Biotechnology. Antibodies against *β*-actin were acquired from Sigma (St. Louis, MO). Horseradish peroxidase (HRP)-conjugated secondary antibodies were purchased from Sigma. Fas siRNA (h, sc-29311), a pool of three target-specific 20−25-nucleotide siRNA designed to knock down Fas gene expression, was purchased from Santa Cruz Biotechnology. The siRNA −A (sc-37007), a nontargeting 20−25-nucleotide species, was used as a negative control.

Cell Culture. SV-40/adenovirus-transformed HLE B-3 cells were a generous gift from U. P. Andley (Department

of Ophthalmology and Visual Sciences, Washington University, St. Louis, MO). The cells were received at passage 14 and were maintained in MEM (Mediatech) containing 20% FBS (Gibco, Carlsbad, CA) and 50 μg/mL gentamicin at 37 °C in 5% CO_2. Cultures were passaged twice per week.

Stable Transfection with hGSTA4. Preparation of hGSTA4-4 eukaryotic expression constructs and transfection of HLE B-3 cells with empty pTarget or pTarget/*hGSTA4* expression vectors were performed using the ProFection Mammalian Transfection kit (Promega) as described previously (*29*).

Transient Transfection with hGSTA4. HLE B-3 cells at a density of 8×10^5 cells per 100 mm Petri dish were plated the day before the transfection. Petri dishes having >50% confluent cells were used for the transfection. The cells were transfected with 10−20 μg of supercoiled plasmid DNA (with empty pTarget or pTarget/*hGSTA4* expression vectors) by using the ProFection Mammalian Transfection kit (Promega) according to the manufacturer's instructions. After 15 h, the cells were treated with 10% DMSO (3 mL per plate) for 2 min. Following the DMSO shock, cells were allowed to recover in complete growth medium. Cells were harvested 24, 48, 72, and 240 h post-transfection, and expression of hGSTA4-4 and Fas was assessed in cell extracts by Western blot analysis.

Transfection of Fas siRNA in HLE B-3 Cells. The Fas siRNA transfection was essentially carried out according to the manufaturer's instructions. Briefly, HLE B-3 cells (2×10^5 cells per well) were plated in a six-well tissue culture plate, in 2 mL of normal growth medium supplemented with FBS. Cells were incubated at 37 °C in a 5% CO_2 incubator until the cells were 60−80% confluent. For each transfection, 50 pmol of siRNA was diluted with 100 μL of siRNA transfection medium (solution A), and 6 μL of siRNA transfection reagent was diluted with 100 μL of siRNA transfection medium (solution B). Solution A was directly added to solution B and the mixture mixed gently, and the mixture was incubated for 30 min at room temperature. Cells were washed with 2 mL of siRNA transfection medium, and 0.8 mL of siRNA transfection medium was added to the mixture of solutions A and B, gently mixed, overlaid on the washed cells, and incubated for 24 h at 37 °C. After 24 h, 2 mL of fresh normal medium was added to each well and cells were incubated for a further 48 h. Control cells were treated in a similar manner with a mixture of scrambled siRNA. Cells were harvested at appropriate time points, and the silencing of Fas was examined by Western blot analysis.

HPLC Analysis of 4-HNE. WT, VT, and *hGSTA4*-transfected (both transiently and stably transfected) cells were suspended in PBS (1 mL) and sonicated (3×10 s, 30 W) on ice. Cell lysates were treated with ice-cold 70% perchloric acid (2 mL) to precipitate proteins and centrifuged at 10000*g* for 10 min. The supernatants were extracted with 2 mL of dichloromethane (HPLC-grade) by gentle vortexing and centrifuged at 1500 rpm for 10 min. The organic layer was collected, dried under nitrogen, resuspended in 100 μL of ethanol, and filtered through nylon 66 filters (Micron Separations Inc.). HPLC analysis of the filtrate was performed on Beckman Coulter System Gold HPLC equipment connected to a Beckman 168 photodiode array (PDA) detector, using a Beckman Ultrasphere (5 μm, 4.6 cm $\times$ 25 cm) column and 70% sodium phosphate (pH 2.6) and 30%

acetonitrile as the mobile phase. 4-HNE in the column eluate was monitored at 202 and 224 nm (*35*).

Preparation of Cell and Tissue Extracts. Cells were pelleted at 2000 rpm, washed twice with cold PBS, and resuspended in radioimmunoprecipitation assay (RIPA) buffer containing 1× PBS (pH 7.4), 1% Nonidet P-40 (NP-40) or Igepal CA-630, 0.5% sodium deoxycholate, 0.1% SDS, 1 mM phenylmethanesulfonyl fluoride (PMSF), and 2 μg/mL pepstatin. To prepare cytoplasmic protein extracts, cells were washed with ice-cold PBS and resuspended in hypotonic lysis buffer (Imgenex) for 15 min, mixed with 30 μL of 10% NP-40, and vortexed for 10 s. The cell lysate was centrifuged for 30 s at 14 000 rpm, and the supernatant was collected for further analyses. To prepare tissue extracts, mouse brain, heart, lung, liver, and kidney were quickly removed after the animal had been sacrificed and immediately transferred to −80 °C until they were used. The tissue samples were washed with 20 mM potassium phosphate (pH 7.0) and 1.4 mM β-mercaptoethanol, homogenized in ice-cold RIPA buffer (3 mL/g of tissue) containing 30 μL of PMSF (10 mg/mL), incubated on ice for 30 min, and centrifuged at 10000g for 10 min. Protein concentrations of cells and tissue extracts were determined by the method of Bradford (*36*).

Western Blot Analysis. Cell extracts containing 30−60 μg of protein were separated on SDS−polyacrylamide (Bio-Rad) gels (10 to 20%) and transferred onto a nitrocellulose membrane (Bio-Rad). Membranes were blocked with 1% fat-free milk and 1% BSA at room temperature for 30 min and incubated overnight at 4 °C with the appropriate primary antibody in 1% milk and 1% BSA in Tris-buffered saline (TBS) containing 50 mM NaF and 0.05% Tween 20 (T-TBS). After being washed with T-TBS, the membrane was incubated with the appropriate secondary antibody at room temperature for 1 h. After being washed again with T-TBS, the membrane was treated with Supersignal "West Pico" chemiluminescent reagent (Pierce) following the manufacturer's instructions and exposed to Hyperfilm ECL film (Amersham) at room temperature.

Detection of PARP. For the detection of PARP, 1×10^7 cells were suspended in 100 μL of denaturing lysis buffer containing 62.5 mM Tris-HCl (pH 6.8), 6.0 M urea, 2% SDS, 10% glycerol, 1.4 mM β-mercaptoethanol, 0.00125% bromophenol blue, 0.5% Triton X-100, and 1 mM PMSF. Cells were sonicated (3×5 s) on ice to disrupt protein−DNA interactions and incubated at 65 °C for 15 min. Samples containing 30 μg of protein were applied to 10% SDS−PAGE gels, and Western blot analysis was performed using PARP monoclonal antibody (clone C2-10, PharMingen, San Diego, CA).

Caspase Assay for in Situ Apoptosis. HLE B-3 wild-type, vector-transfected, or *hGSTA4*-transfected cells (1×10^5) were treated with 20 μM 4-HNE for 0.5 and 2 h at 37 °C. Apoptotic cells were detected by staining with 10 μM CaspACE FITC-VAD-FMK (Promega) *in situ* marker for 30 min in the dark. The slides were rinsed with PBS twice, fixed with 4% paraformaldehyde for 1 h, mounted in a medium containing DAPI (1.5 μg/mL), and observed under a fluorescence microscope (Olympus).

Immunohistochemical Localization of Fas. For immunohistochemical localization of Fas, cells were grown in chamber slides and fixed in 4% paraformaldehyde for 20 min at room temperature followed by washing twice with PBS. The cells were incubated with primary anti-Fas (B-10) mouse monoclonal IgG (5 μg/mL, in PBS containing 1% BSA) for 2 h at room temperature in a humidified chamber. The primary antibody was washed off with PBS (10 min). Secondary goat anti-mouse FITC-conjugated antibody (3 μg/mL, in PBS containing 1% BSA) was added, and incubation was carried out for 1 h at room temperature. Unbound secondary antibody was removed by washing with PBS (10 min). Slides were mounted with cover slips with Vectashield DAPI mounting medium (Vector Laboratories, Inc., Burlingame, CA) and photographed at 400× magnification using a LEICA DMLB fluorescence microscope.

Localization of Fas in Tissues. Paraffin-embedded tissue sections were deparaffinized by being placed in xylene for 20 min at room temperature. The tissues were hydrated in a graded series of ethanol (100, 95, 70, 50, and 30% in water) for 10 min each and equilibrated in PBS. The slides were incubated with anti-Fas primary antibody (B-10, mouse monoclonal IgG, 5 μg/mL in PBS containing 1% BSA) for 2 h at room temperature in a humidifier chamber. The primary antibody was washed off with PBS (10 min). Goat anti-mouse FITC-conjugated antibody (3 μg/mL, in PBS containing 1% BSA) was added. After 1 h at room temperature, unbound secondary antibody was removed by washing with PBS (10 min), and slides were mounted with cover slips with Vectashield DAPI mounting medium and analyzed under a fluorescence microscope using a standard fluorescence filter set to view the green fluorescence of FITC at 520 ± 20 nm and the blue fluorescence of DAPI at 460 nm. Photographs were taken at 400× magnification.

Immunoprecipitation Studies. Cells were washed twice with cold PBS, and pellets were resuspended in RIPA buffer containing 1× PBS (pH 7.4), 1% NP-40 or Igepal CA-630, 0.5% sodium deoxycholate, 0.1% SDS, 1 mM phenylmethanesulfonyl fluoride, and 2 μg/mL pepstatin. Following sonication on ice, the homogenates were centrifuged at 14000g for 15 min at 4 °C, and aliquots of the supernatant containing 500 μg of protein were incubated with anti-Fas antibodies (1:100) at 4 °C overnight; 50 μL of protein A/G−agarose beads was then added to the reaction mixture and the mixture incubated again overnight at 4 °C. The agarose beads were collected by pulse centrifugation (5 s at 14 000 rpm), washed three times with ice-cold RIPA buffer, resuspended in 60 μL of 2× sample buffer, and boiled for 5 min to dissociate the immunocomplexes from the beads. The supernatant collected after centrifugation (14 000 rpm) was subjected to Western blot analysis using specific antibodies.

RESULTS

4-HNE Causes Induction of Fas. Previous studies (*28*, *29*) have shown that depletion of 4-HNE in HLE B-3 cells by overexpression of the 4-HNE-metabolizing GST isozyme hGSTA4-4 results in the transformation of the cells along with an irreversible and complete suppression of Fas expression in the transformed cells. While these findings implicate 4-HNE in the regulation of Fas expression, it is not clear whether the suppression of Fas expression upon 4-HNE depletion precedes the transformation or whether it is a consequence of the transformation. Therefore, we systematically examined the expression of Fas under various condi-
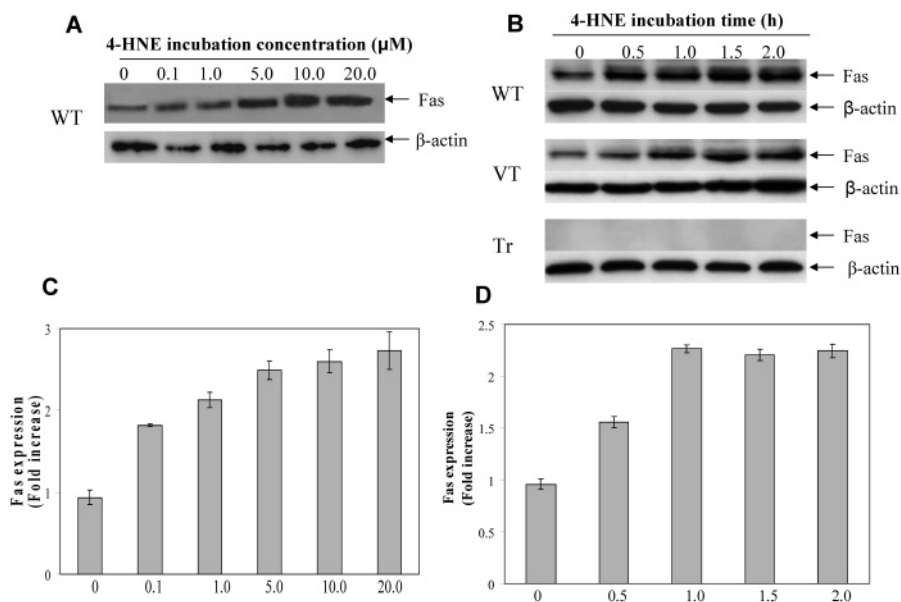
FIGURE 1: Effect of 4-HNE on Fas expression in HLE B-3 cells. (A) HLE B-3 wild-type (WT) cells in complete growth medium were treated with different concentrations of 4-HNE (from 0 to 20 μM) for 2 h. (B) HLE B-3 wild-type (WT), vector-transfected (VT), and *hGSTA4*-transfected (Tr) cells were treated with 4-HNE (20 μM) for different periods of time (0, 0.5, 1.0, 1.5, and 2 h). The cells were homogenized in RIPA buffer and centrifuged at 14 000 rpm. Supernatants containing 60 μg of protein from WT, VT, and Tr cells were subjected to Western blot analysis using anti-Fas monoclonal antibodies (B-10) as described in Materials and Methods. Blots were developed with West Pico-chemiluminescence reagent (Pierce). β-Actin blot was used as a loading control. Representative immunoblots are presented in both panels A and B. (C and D) Bar graphs showing the densitometric analysis (Kodak 1D 3.6 software) of the bands from immunoblots obtained from three different experiments (mean $\pm$ standard deviation; $n = 3$).
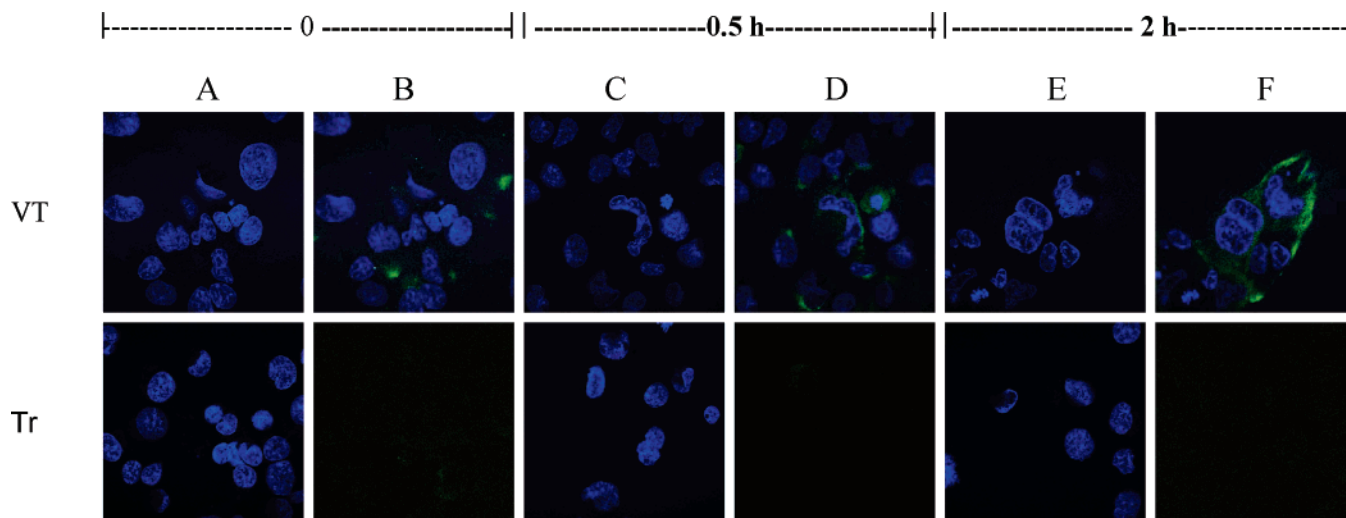

FIGURE 2: Immunofluorescence of Fas expression in HLE B-3 cells. VT and Tr HLE B-3 cells (5×10^4 cells per chamber) were grown in chamber slides in complete growth medium and were treated with 20 μM 4-HNE for 0, 0.5, and 2 h. After being treated, the cells were fixed in 4% paraformaldehyde and then incubated with primary anti-Fas (B-10) mouse monoclonal IgG for 2 h. Secondary goat anti-mouse FITC-conjugated antibodies were added, and incubation was further carried out for 1 h at room temperature. Slides were mounted with cover slips using Vectashield DAPI mounting medium. The slides were viewed with a fluorescence microscope using a standard fluorescence filter set to view blue (DAPI, panels A, C, and E) and green fluorescence (Fas-FITC, panels B, D, and F). The photographs were taken at 400× magnification.

tions affecting the intracellular concentration of 4-HNE. When HLE B-3 cells were incubated for 2 h with gradually increasing concentrations of 4-HNE (0.1–20 μM), a dose-dependent increase in the level of expression of Fas was observed with optimal induction by 20 μM 4-HNE (Figure 1A). Western blot analyses presented in Figure 1B show that incubation with 20 μM 4-HNE caused a time-dependent increase in the level of expression of Fas in wild-type (WT) as well as in empty vector-transfected (VT) cells. A >2-fold induction of Fas was observed in these cells after incubation for 2 h with 20 μM 4-HNE (Figure 1C,D). On

the other hand, Fas was not detected in untreated as well as 4-HNE-treated *hGSTA4*-transfected transformed cells which constitutively lack Fas expression (*29*). An increased level of expression of Fas in 4-HNE-treated HLE B-3 WT and VT cells was confirmed by confocal microscopy (Figure 2). As expected, in these cells Fas was localized to the plasma membrane. The confocal microscopy findings were consistent with the results of Western blot analyses (Figure 1). Together, these results show that an increase in the intracellular concentration of 4-HNE upregulates the expression of Fas in HLE B-3 cells.
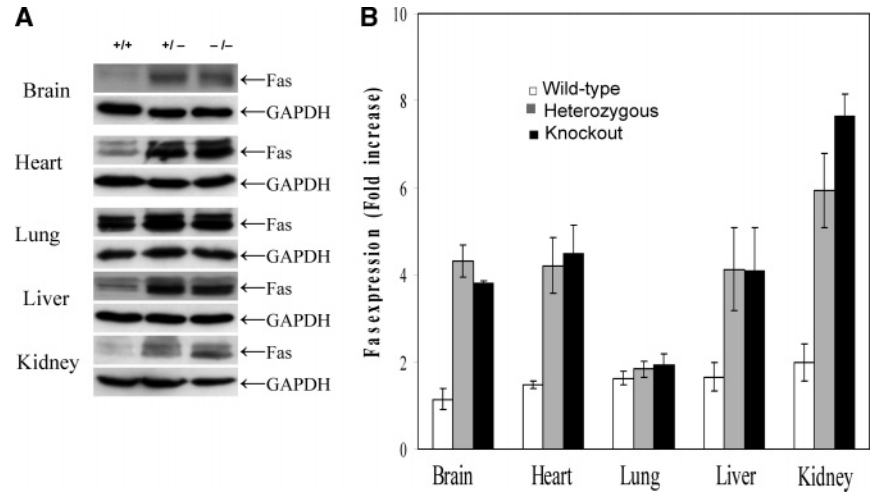
FIGURE 3: Expression of Fas in different tissues of *mGSTA4* (+/+), (+/−), and (−/−) mice. (A) Mouse brain, heart, lung, liver, and kidney tissues were homogenized in ice-cold RIPA buffer and centrifuged at 14 000 rpm. Supernatants (30 μg of protein) were loaded on a 10 to 20% polyacrylamide gel. Fas expression was monitored by Western blot analysis using anti-Fas monoclonal antibodies (B-10) (1:200). GAPDH was used as a loading control. Blots were developed with West Pico-chemiluminescence reagent (Pierce). (B) Bar chart showing densitometric analysis (Kodak 1D 3.6 software) of bands from immunoblots of three different experiments (mean $\pm$ standard deviation; $n = 3$).
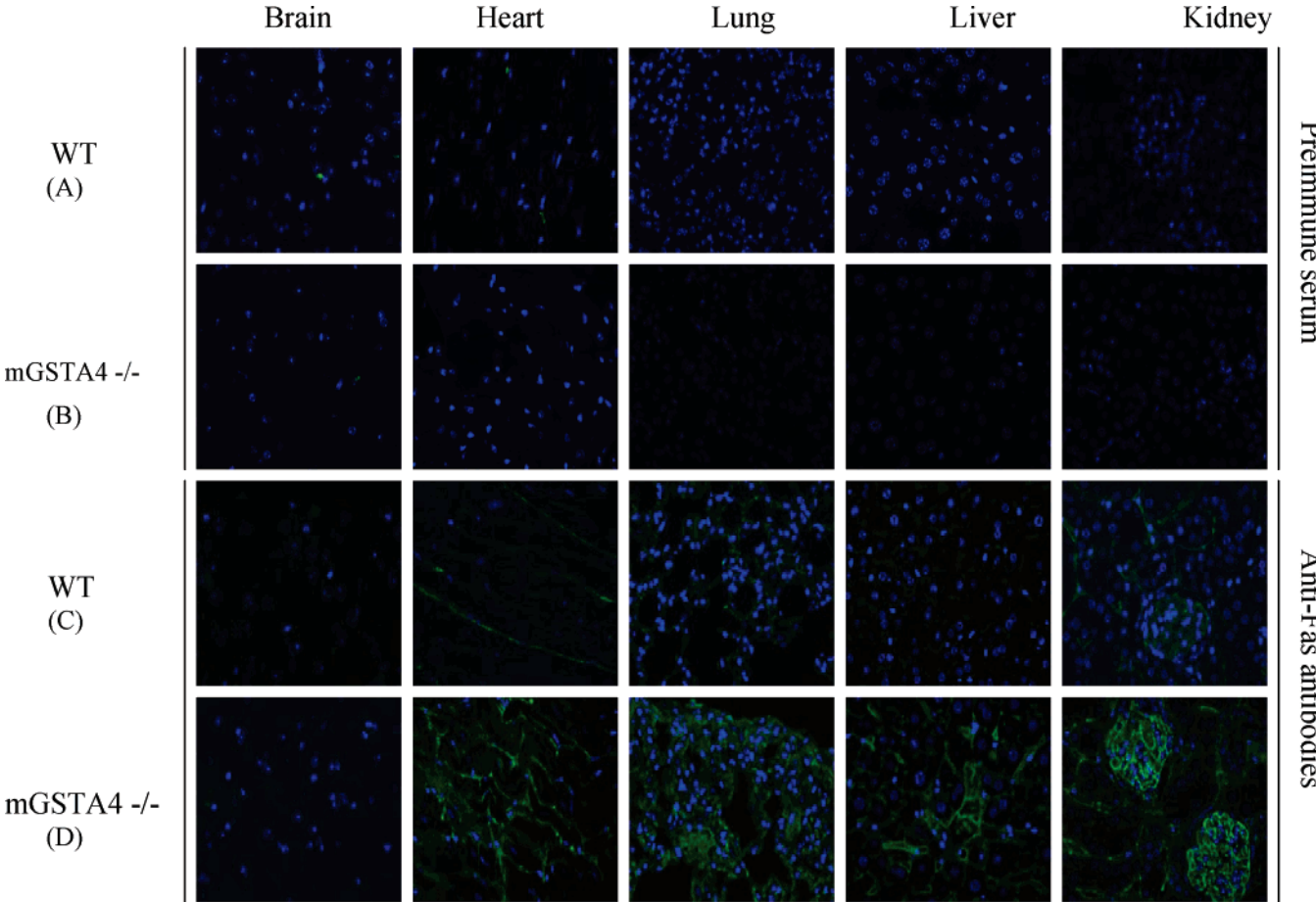

FIGURE 4: Localization of Fas in different tissues of *mGSTA4* (+/+) and (−/−) mice. Paraffin-embedded tissue sections were deparaffinized by placing them in xylene for 20 min at room temperature. The tissues were hydrated in a graded series of ethanol and equilibrated in PBS. The slides were incubated with primary anti-Fas (B-10) mouse monoclonal IgG (5 μg/mL, in PBS containing 1% BSA) for 2 h at room temperature. Secondary antibody goat anti-mouse FITC (3 μg/mL, in PBS containing 1% BSA) was added and incubation carried out for 1 h at room temperature. Slides were mounted with cover slips with Vectashield DAPI mounting medium. Slides were analyzed under a fluorescence microscope (Olympus) using a standard fluorescein filter set to view the blue fluorescence (DAPI) and green fluorescence (FITC). The photographs were taken at 400× magnification. All panels show a combined view of the DAPI and FITC stains. (A and B) WT and *mGsta4* null mice tissues treated with whole mouse IgG used as negative controls. (C and D) Tissues from WT and *mGsta4* null mice treated with anti-Fas antibodies.

Increased 4-HNE Levels in Mouse Tissues Lead to Fas Induction. The *in vitro* cell culture studies presented above were extended to *in vivo* conditions using the tissues from *mGsta4* null mice which have been shown to contain an approximately 3-fold higher concentration of 4-HNE, at least in liver (*33*). To test the hypothesis that the increase in the level of Fas expression in response to higher 4-HNE levels observed in cultured cells is also reflected *in vivo*, we compared the expression of Fas in the tissues of *mGsta4* (−/−), (+/−), and wild-type (+/+) mice. Consistent with our prediction, results of Western blot analysis presented in Figure 3 show that Fas expression was remarkably upregulated in all tissues of *mGsta4* (−/−) and (+/−) mice examined in this study. Increased 4-HNE levels seem to differentially affect Fas expression in the tissues of (−/−) and (+/−) mice. A more pronounced increase was observed in the liver and heart of (−/−) and (+/−) mice as compared to that in the brain and lung. Particularly in liver, where basal levels of Fas expression were low, the level of induction was noticeably high. On the other hand, the level of induction in lung was low as lung had higher constitutive levels of Fas than liver, brain, heart, or kidney. These results, confirmed by immunohistochemical analyses presented in Figure 4, demonstrate for the first time that in an *in vivo* model, the expression of Fas is modulated by 4-HNE and that the intracellular concentration of 4-HNE may be a determinant for the level of Fas expression. Furthermore, these results also indicate that 4-HNE-mediated regulation of Fas is not limited to a specific cell type but appears to be a generalized phenomenon.

Downregulation of Fas Expression upon 4-HNE Depletion. We have consistently observed that the expression of hGSTA4-4 in HLE B-3 cells transiently transfected with *hGSTA4* was optimal during the period between 48 and 72 h post-transfection. Subsequently, the hGSTA4-4 level gradually declined with an almost complete loss of expression on day 10 post-transfection. To evaluate the effect of transient hGSTA4-4 expression on the intracellular levels of 4-HNE, we compared the 4-HNE levels of HLE B-3 cells transiently transfected with *hGSTA4* with those of the corresponding control at different time periods. Results of the HPLC analysis for 4-HNE determination presented in Figure 5B show that the intracellular 4-HNE concentrations in GSTA4-4-expressing cells remained significantly lower (55−65%) than those of control cells at least up to 72 h post-transfection. This was consistent with the results of Western blot analysis which showed that transiently transfected cells overexpressed hGSTA4-4 for at least 72 h (Figure 5A). Unlike cells stably transfected with *hGSTA4* (*29*), transiently transfected cells did not undergo transformation or any observable morphological changes. Concomitant with lower 4-HNE levels, expression of Fas in these cells was suppressed at 48 and 72 h post-transfection (Figure 5A). Ten days after transfection, when hGSTA4-4 expression was lost, both the 4-HNE concentration and the level of Fas expression returned to their respective basal levels. These results indicate that lowering of the intracellular concentration of 4-HNE leads to suppression of Fas expression and are consistent with the notion that 4-HNE is an important determinant of the level of Fas expression. Furthermore, these results show that a complete attenuation of Fas expression in HLE B-3 cells transformed by stable transfection of *hGSTA4* reported
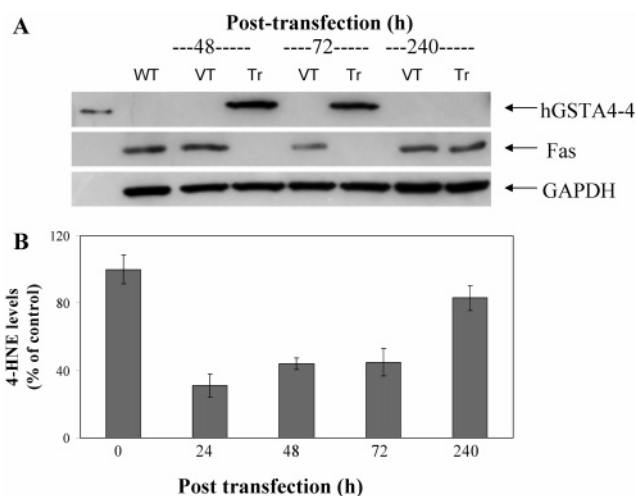

FIGURE 5: Expression of Fas and hGST A4-4 in HLE B-3 cells transiently transfected with *hGSTA4*. (A) Cells (1×10^6), wild type (WT), transiently transfected with *hGSTA4* (Tr), or transiently transfected with empty vector (VT), were pelleted and sonicated in ice-cold RIPA buffer. Supernatants containing 30 μg of protein were subjected to Western blot analysis as described in Materials and Methods. Monoclonal antibodies against mouse Fas (B-10) (1: 200) and hGSTA4-4 polyclonal chicken antibodies (1:5000) were used as primary antibodies. HRP-conjugated anti-mouse (1:1000) and anti-chicken (1:10000) antibodies were used as secondary antibodies. GAPDH was used as loading control. Blots were developed with West Pico-chemiluminescence reagent (Pierce). (B) Intracellular concentration of 4-HNE in transiently *hGSTA4*-transfected HLE B-3 cells. VT and Tr cells were harvested 24, 48, 72, and 240 h post-transfection. Cell pellets were immediately suspended in PBS (1 mL), sonicated on ice (3×10 s, 30 W), then treated with ice-cold 70% perchloric acid (2 mL), centrifuged to remove denatured protein, and extracted with 2 mL of dichloromethane. The organic layer was collected and dried under nitrogen. The residue was dissolved in a fixed volume of ethanol and filtered through a nylon filter. The ethanol extract was subjected to HPLC analysis using a RPC18 column the same day as described in the text. The elution of 4-HNE was monitored at 224 and 202 nm. The intracellular concentration of 4-HNE was calculated with a calibration graph prepared by using different concentrations of standard 4-HNE. The bar chart shows the mean ± standard deviation ($n = 3$).

previously (*28*) is probably not a consequence of transformation since a decrease in the level of Fas expression upon 4-HNE depletion precedes the transformation of cells.

Fas-Deficient Cells Are Protected against 4-HNE-Induced Apoptosis. 4-HNE is known to cause apoptosis in various cell lines, including HLE B-3 cells (*30−32*). When treated with 20 μM 4-HNE for 2 h, the WT and VT HLE B-3 cells exhibited significant apoptosis as indicated by the activation of caspase (Figure 6, top and middle panels). On the other hand, *hGSTA4*-transfected transformed HLE B-3 cells which do not express any detectable Fas (*28*) were resistant to apoptosis under these conditions (Figure 6, bottom panel). Sustained activation of JNK (Figure 7B) has been shown to precede apoptosis in a variety of cells (*14*, *20*, *32*). As shown in Figure 7A, JNK was activated in VT HLE B-3 cells upon 4-HNE treatment. Likewise, JNK activation was also observed in 4-HNE-treated WT cells (data not presented). In contrast, *hGSTA4*-transfected cells neither underwent apoptosis (Figure 6, bottom panel) nor exhibited any significant activation of JNK (Figure 7B) upon 4-HNE treatment. In VT or WT cells, the activation of caspase was also indicated by significant cleavage of PARP which was not observed in
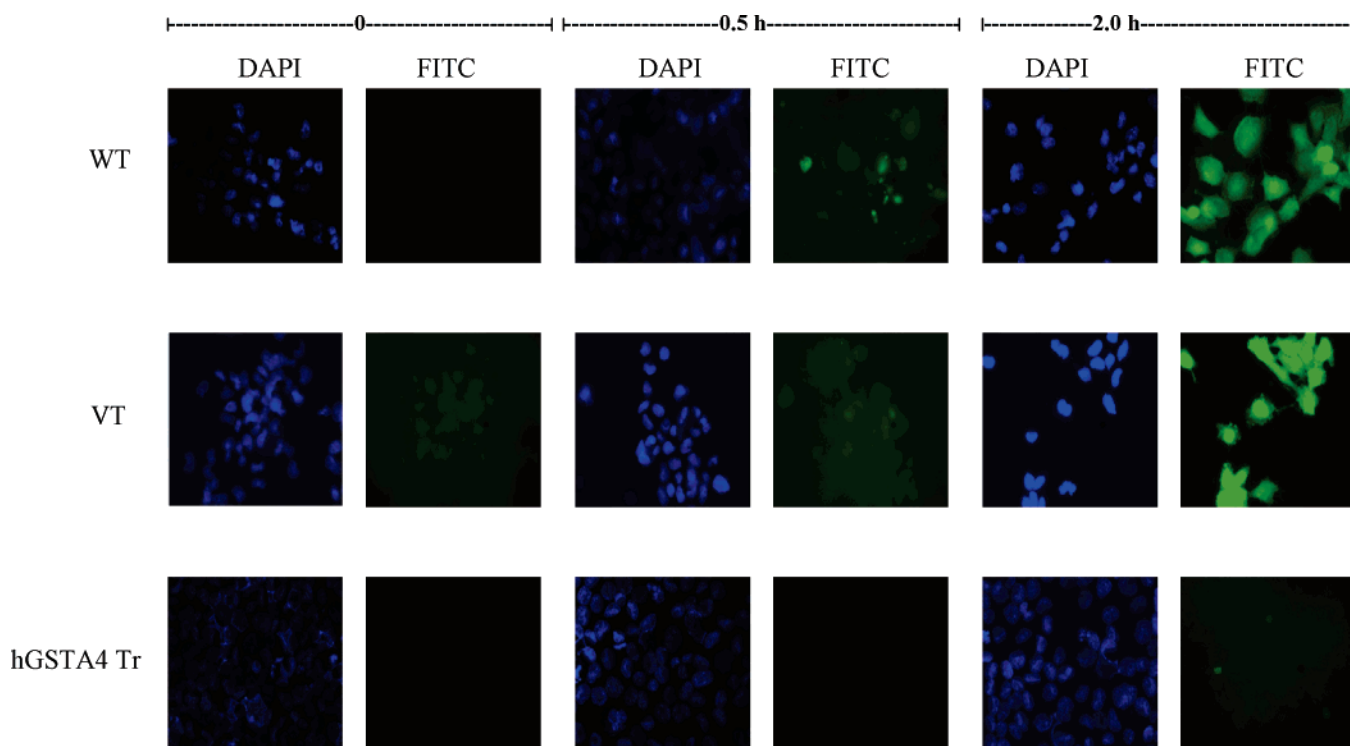
FIGURE 6: *In situ* analysis of activated caspase 3 in HLE B-3 cells. WT (top row), VT (middle row), and Tr (bottom row) cells (5×10^4) were grown in chamber slides in serum-free medium and treated with 4-HNE (20 μM) for 0, 0.5, and 2 h. The activation of caspase in these cells was examined by staining with 10 μM CaspACE FITC-VAD-FMK *in situ* marker following the manufacturer's instructions. The slides were mounted with Vectashield DAPI mounting medium and observed with a fluorescence microscope (Olympus) using standard filter sets for DAPI and FITC. The photographs were taken at 400× magnification. Green FITC-labeled WT and VT cells show a time-dependent increase in the level of caspase 3 activation after 4-HNE treatment. Different panels show blue DAPI-stained and green FITC-stained cells as marked in the figure.
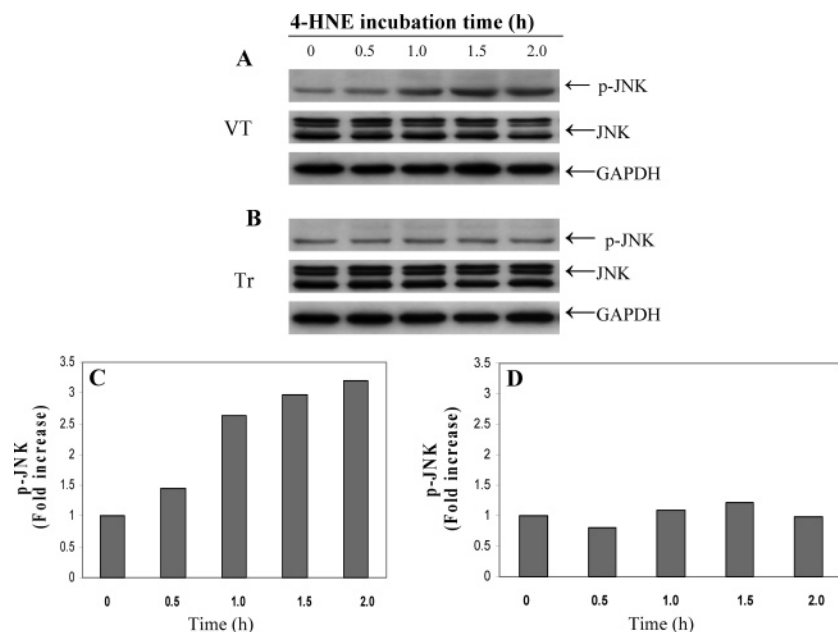

FIGURE 7: Expression of JNK and p-JNK in HLE B-3 cells treated with 4-HNE. VT (A) and Tr (B) cells (2×10^5 cells/60 mm dish) in complete growth medium were treated with 20 μM 4-HNE for 0, 0.5, 1, 1.5, and 2 h. The cells were then pelleted and homogenized in lysis buffer containing 50 mM Tris-HCl (pH 7.5), 1 mM sodium orthovanadate, 50 mM NaF, 20 μg/mL PMSF, 4 mM EDTA, 1 mM EGTA, 1% NP-40, 150 mM sodium chloride, 100 μM leupeptin, 0.07 μg/mL pepstain, 10 μg/mL soybean trypsin inhibitor (T9003, Sigma), 1:100 protease inhibitor cocktail (P2714, Sigma), and 1:100 phosphatase inhibitor cocktail (P5726, Sigma) and centrifuged at 14 000 rpm. Supernatants containing 30 μg of protein were subjected to Western blot analysis using anti-p-JNK and anti-JNK monoclonal antibodies. GAPDH was used as a loading control. Blots were developed with West Pico-chemiluminescence reagent (Pierce). Representative blots from three different experiments yielding similar results are presented. Panels C and D present the bar graphs showing results of densitometric analysis (Kodak 1D 3.6 software) of bands in panels A and B.

hGSTA4-transfected cells (Figure 8). These results show that *hGSTA4*-transfected cells lacking the expression of Fas are resistant to apoptosis caused by 4-HNE and suggest a role of Fas in 4-HNE-induced apoptosis in HLE B-3 cells.
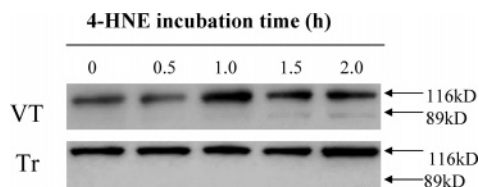
FIGURE 8: Activation of PARP in HLE B-3 cells treated with 4-HNE. VT and Tr cells (2×10^5 cells/60 mm dish) in complete medium were treated with 20 μM 4-HNE for 0, 0.5, 1, 1.5, and 2 h. The cells were pelleted and then suspended in 100 μL of denaturing lysis buffer containing 62.5 mM Tris-HCl, 6 M urea (pH 6.8), 2% SDS, 10% glycerol, 1.4 mM β-mercaptoethanol, 0.00125% bromophenol blue, 0.5% Triton X-100, and 1 mM PMSF. Cells were sonicated for 3×5 s on ice to disrupt protein−DNA interaction, incubated at 65 °C for 15 min, and centrifuged at 14 000 rpm. Supernatants (30 μg) were applied to 12% SDS−PAGE gels, and Western blot analysis was performed using PARP monoclonal antibodies. Blots were developed with West Pico-chemiluminescence reagent.
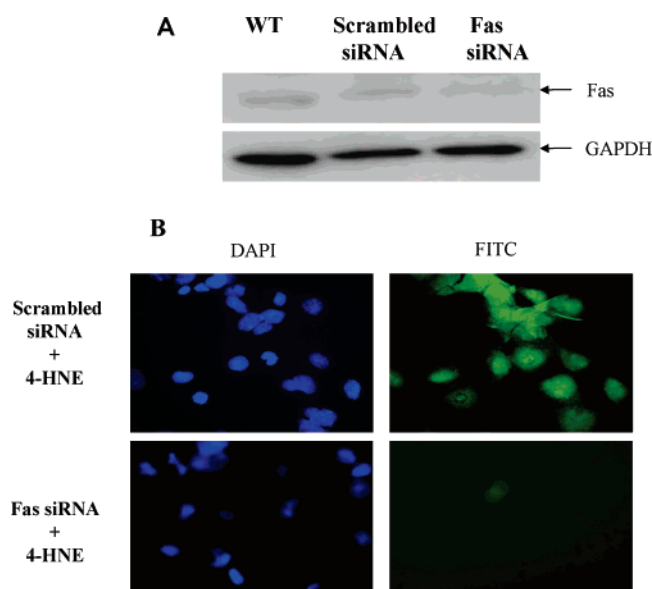

FIGURE 9: Effect of 4-HNE on HLE B-3 cells transfected with Fas siRNA. WT HLE B-3 cells (2×10^5) per well were plated in a six-well plate in complete growth medium and incubated until they were 60−80% confluent. Cells were transfected with Fas siRNA duplex (50 pmol) detailed in Materials and Methods. Control cells were treated with the scrambled siRNA duplex in the similar manner. (A) Cells were harvested 72 h post-transfection, and depletion of Fas was examined by Western blot analysis of the cell extracts prepared in RIPA buffer using anti-Fas (B-10) antibodies. (B) After we ascertained depletion of Fas, the cells (4×10^4) grown in chamber slides were treated with 4-HNE (20 μM) for 2 h, after which 4-HNE-containing medium was removed and the cells were immediately treated with CasACE-FITC-VAD-FMK *in situ* marker following the manufacturer's instructions. The cells were washed, fixed, and processed as described in Materials and Methods. Slides were viewed immediately under a fluorescence microscope (Olympus) using standard filter sets for DAPI and FITC as indicated in cells transfected with scrambled or Fas siRNA as marked in the figure. Results of the analysis of an experiment done in triplicate are shown.

Effect of Fas siRNA on 4-HNE-Induced Apoptosis. The involvement of Fas in 4-HNE-induced apoptosis was further suggested by results of experiments with Fas siRNA-transfected HLE B-3 cells. As shown in Figure 9A, Fas siRNA-transfected cells expressed barely detectable levels of Fas as opposed to the WT or those transfected with scrambled siRNA. Upon 4-HNE treatment, Fas-depleted cells

were found to be relatively more resistant to 4-HNE-induced apoptosis than the WT or scrambled siRNA-treated Fas positive cells (Figure 9B). These results further suggested an at least partial role of Fas in 4-HNE-induced apoptosis.

Increased Intracellular 4-HNE Levels in Mouse Tissues Cause JNK Activation. Since *in vitro* studies carried out with both WT and VT HLE B-3 cells showed a sustained activation of JNK after being treated for 30 min with 20 μM 4-HNE, we examined whether the expression of JNK was upregulated in the liver, heart, lung, and brain tissues of *mGsta4* (−/−) mice due to the enhanced ambient concentration of 4-HNE. The results presented in Figure 10 indicate that JNK was indeed activated in all examined tissues of *mGsta4* (−/−) mice as compared to the (+/+) mice.

Mechanism of 4-HNE-Induced Apoptosis in HLE B-3 Cells. The canonical pathway through which Fas signals apoptosis involves its interaction with FADD (*37*). Fas receptor has two different functional regions, a pre-ligand association domain located on the cell membrane and a death domain (DD) in its cytoplasmic tail. When the cell enters apoptosis, the Fas receptor combined with Fas L causes its death domain to recruit FADD, procaspase 8, procaspase 10, and c-FLIP to assemble the death-inducing signaling complex (DISC) which directs the activation of the downstream caspases (*37*). To investigate whether this pathway was involved in 4-HNE-induced apoptosis, HLE B-3 cells were treated with 20 μM 4-HNE for 2 h, and Fas antibodies were used to immunoprecipitate the DISC components. The immunoprecipitates obtained from the control and 4-HNE-treated cells were probed for FADD, Fas L, and procaspase 8 using respective specific antibodies against these proteins. Results of these experiments presented in Figure 11 showed that while Fas L, FADD, and procaspase 8 were detected in cell lysate (Figure 11, left panel), none of these proteins were either induced upon 4-HNE treatment or immunoprecipitated with Fas antibodies (Figure 11, right panel). These results suggest that 4-HNE-induced apoptosis of HLE B-3 cells does not involve Fas L and FADD as reported for the canonical DISC pathway demonstrated in other cell types.

Another receptor-associated protein, Daxx, has also been implicated in the mechanisms of Fas-mediated apoptosis through a pathway which is independent of the Fas−FADD−DISC cascade (*38−40*). Daxx is primarily a nuclear protein which, upon translocation to the cytosol, binds to specific death domains of Fas and causes activation of apoptosis by regulating kinase 1 (ASK1) and JNK. To investigate whether Daxx was involved in 4-HNE-induced apoptosis of HLE B-3 cells, we examined the effect of 4-HNE on Daxx. Results presented in Figure 12A showed that Daxx was induced in the cytosol of the WT HLE B-3 cells upon 4-HNE treatment. Furthermore, in immunoprecipitation experiments, Daxx was immunoprecipitated by Fas antibodies, indicating the binding of Daxx to Fas (Figure 12B). Activation of ASK1 has also been reported during Fas−Daxx-mediated apoptosis (*39*). However, we did not observe any noticeable activation of ASK1 (data not presented).

DISCUSSION

Results presented here demonstrate for the first time that the expression and functions of Fas can be modulated by
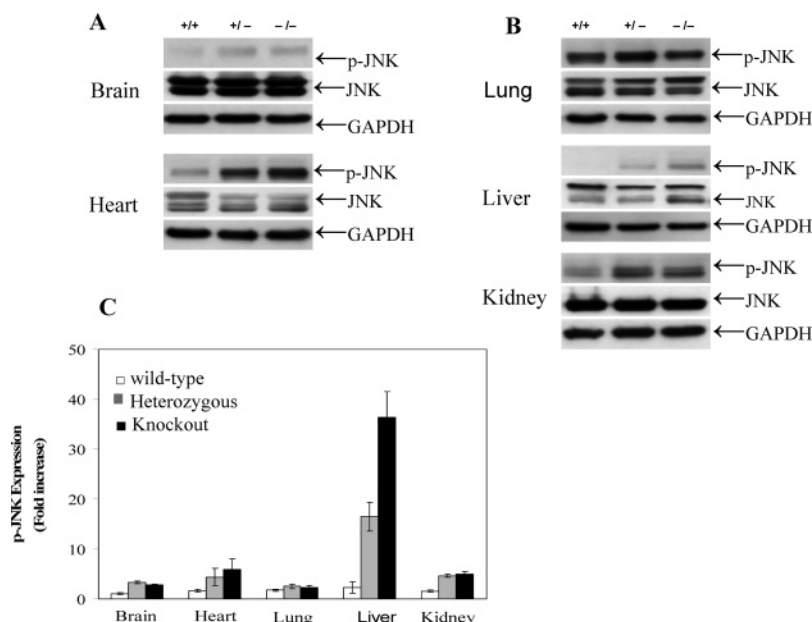
FIGURE 10: Expression of JNK and p-JNK in different tissues of *mGSTA4* (+/+), (+/−), and (−/−) mice. Mice brain, heart (A), lung, liver, and kidney (B) were homogenized in lysis buffer containing 50 mM Tris-HCl (pH 7.5), 1 mM sodium orthovanadate, 50 mM NaF, 20 μg/mL PMSF, 4 mM EDTA, 1 mM EGTA, 1% NP-40, 150 mM sodium chloride, 100 μM leupeptin, 0.07 μg/mL pepstain, 10 μg/mL soybean trypsin inhibitor (T9003, Sigma), 1:100 protease inhibitor cocktail (P2714, Sigma), and 1:100 phosphatase inhibitor cocktail (P5726, Sigma) and centrifuged at 14 000 rpm. Supernatants (30 μg of protein) were loaded on a 12% polyacrylamide gel. p-JNK and JNK were assayed by Western blot analysis using anti-p-JNK and anti-JNK monoclonal antibodies. GAPDH was used as a loading control. Blots were developed with West Pico-chemiluminescence reagent (Pierce). (C) Bar chart showing the densitometric analysis (Kodak 1D 3.6 software) of bands of immunoblots from three different experiments (mean ± standard deviation; $n = 3$).
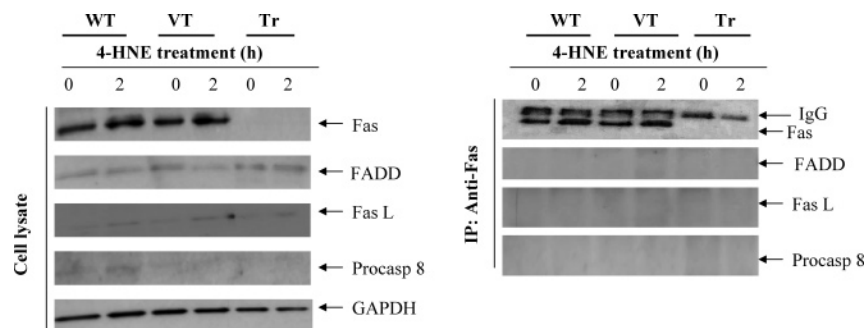

FIGURE 11: Immunoprecipitation of Fas, FADD, Fas L, and procaspase 8 in HLE B-3 cells. WT, VT, and Tr cells in complete growth medium were treated with 20 μM 4-HNE for 2 h. Control cells were treated with an equal volume of vehicle (PBS) alone (0 h treatment). Cells were harvested, washed, and homogenized in RIPA buffer. Aliquots of cell extracts containing 500 μg of protein were immunoprecipitated with anti-Fas monoclonal antibodies (B-10) as described in Materials and Methods. The whole cell lysates (left panel) and the immunoprecipitates (IP, right panel) were analyzed by Western blot analysis using anti-Fas monoclonal, rabbit anti-FADD, rabbit anti-Fas L, or rabbit anti-procaspase 8 antibodies appropriately marked in the figure. GAPDH was used as a loading control. Blots were developed with West Pico-chemiluminescence reagent (Pierce).

4-HNE in a time- and concentration-dependent manner. 4-HNE has been shown to modulate cellular signaling processes, including the induction of apoptosis in a variety of cell lines *in vitro* (*19*, *22*). Recent studies (*15*, *16*, *20*) have suggested that 4-HNE is a common denominator in stress-induced signaling for apoptosis in a variety of cells, including HL60 and K562 (which grow indefinitely in suspension) as well as in HLE B-3 and human retinal pigment epithelial (RPE) cells (which are attached cells with a limited replicative life span). Studies by a diverse group of investigators have shown that 4-HNE can cause activation of adenylate cyclase (*41*), phospholipase C (*42*), SAPKs including JNKs (*13*, *14*), PKC (*27*, *43*), and tyrosine kinases (*21*). 4-HNE can also modulate the expression of various genes involved in regulation of the cell cycle, chemotaxis, apoptosis, and cell proliferation (*19*, *22*). Our recent studies

have shown that lowering the intracellular concentration of 4-HNE results in a profound change in the expression of genes involved in the regulation of cell cycle control and cell−cell adhesion (*28*, *29*). The studies presented here demonstrating the regulation of Fas expression and the pathways through which Fas mediates apoptotic signaling are consistent with the idea that 4-HNE is an important signaling molecule.

Results presented here provide compelling evidence for regulation of Fas expression by 4-HNE in a dose- and time-dependent manner. The results of Western blots as well as immunohistochemical studies show a time-dependent gradual increase in the level of Fas expression in plasma membranes of cells bathed in 4-HNE-containing medium. More importantly, our studies show the dependence of Fas expression *in vivo* on tissue levels of 4-HNE. This is indicated by

A

4-HNE incubation time (h)

0   0.5   1.0   1.5   2.0

WT cytosol ← Daxx

← GAPDH

B

----WT----   -----VT----   ----Tr----

0   2.0   0   2.0   0   2.0h
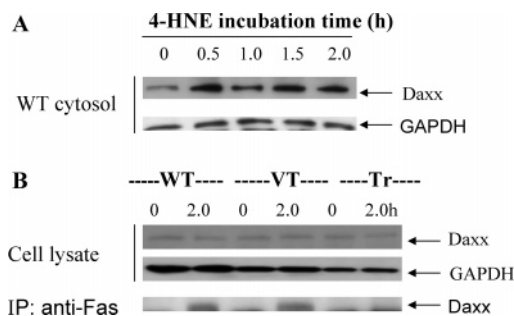
Cell lysate ← Daxx

← GAPDH

IP: anti-Fas ← Daxx

FIGURE 12: Expression of Daxx protein levels in 4-HNE-treated HLE B-3 cells and its immunoprecipitation by anti-Fas antibodies. WT, VT, and Tr cells cultured in complete growth medium were treated with 20 μM 4-HNE and harvested after 2 h. Cytoplasmic and whole cell extracts were prepared using the Imegenex cell processing kit and RIPA buffer, respectively. The whole cell extracts (500 μg of protein) were immunoprecipitated with anti-Fas mono-clonal antibodies as described in the text and then analyzed for Daxx expression by Western blotting. (A) Expression of Daxx in the 4-HNE-treated WT cytoplasmic cell extracts. (B) Immunoblot analysis of 4-HNE-treated WT, VT, and Tr cell immunoprecipitates probed by anti-Daxx polyclonal antibodies.

Western blot studies, as well as by immunohistochemical localization experiments which show significantly enhanced Fas levels in tissues of *mGsta4* null mice which have 2−3-fold higher tissue levels of 4-HNE as compared to the controls (*33*). The physiological significance of these findings is not clear, but Fas upregulation with a concurrent increase in the level of phosphorylated JNK in the tissues of *mGsta4* null mice strongly suggests that some of the signaling proteins downstream of Fas in the apoptosis signaling pathway are also modulated in these mice due to the elevated 4-HNE levels in tissues. Our preliminary studies (*44*) show that *mGsta4* null mice acquire obesity with age. Since recent studies with hepatectomized mice indicate a role of Fas in the proliferation of hepatocytes and accelerated liver regen-eration (*45*), it may be worthwhile to explore a possible link between the obsese phenotype of *mGsta4* null mice and the induction of Fas in tissues of these mice.

In these studies, we have also examined 4-HNE-mediated regulation of Fas expression through an alternative approach by manipulating the intracellular concentration of 4-HNE within the cells. Our results show that in cells transiently transfected with *hGSTA4*, lower 4-HNE levels persist up to 72 h after transfection and that during this period Fas expression is strongly suppressed. This suppression of Fas is most likely due to the depletion of cellular 4-HNE because when the forced expression of *hGSTA4* in these cells ceases 10 days post-transfection, the level of Fas expression and the 4-HNE concentration return to their basal levels. It is well established that the constitutive levels of 4-HNE in cells are low, vary in different cell types and tissues, and are subject to change upon alterations in the redox state of cells (*13, 20*). Our results suggest that even a small change in 4-HNE levels (i.e., lowering by ∼40%) in transfected cells leads to suppression of Fas expression. These results are consistent with our earlier studies (*28, 29*) showing that the expression of some key proteins, including integrin α6 and p53, is almost completely lost in HLE B-3 cells in which subphysiological levels of 4-HNE are maintained by stable transfection with *hGSTA4* leading to their phenotypic transformation (*29*). It could be argued that these observed effects could be due to some nonspecific effects of *hGSTA4*

transfection. However, results of previous studies (*29*) showing that transfection of HLE B-3 cells with a mutant hGSTA4-4 (Y212F), having no significant activity toward 4-HNE, results in neither the transformation of cells nor 4-HNE depletion argue against this possibility. Results presented here also show that suppression of Fas expression in 4-HNE-depleted cells precedes the transformation of HLE B-3 cells upon *hGSTA4* transfection and that the suppression of Fas expression can be reversed in early stages if the basal levels of 4-HNE are restored in cells.

The mechanisms through which Fas and other death receptors of the TNF-α supergene family signal for apoptosis have been studied extensively. We demonstrate that Fas-deficient transformed HLE B-3 cells are resistant to 4-HNE-induced apoptosis. Likewise, cells in which Fas expression is transiently suppressed (up to ∼80%) by siRNA also acquire resistance to 4-HNE-induced apoptosis, suggesting a role of Fas, at least in part, in this process. Previous studies suggest that Fas-mediated signaling for apotosis could be transduced by at least two distinct pathways (*37, 39, 46*). These pathways include the canonical FADD-dependent pathway and the Daxx-dependent pathway, both of which lead to the activation of JNK. Immunoprecipitation experi-ments using Fas antibodies show that Fas L, FADD, and procaspase 8 do not co-immunoprecipitate with Fas in 4-HNE-treated HLE B-3 cells, indicating that 4-HNE-induced apoptosis of HLE B-3 cells does not involve Fas L, FADD, and caspase 8 which are components of the canonical pathway. The induction of Daxx in the cytosol of 4-HNE-treated cells and its immunoprecipitation by Fas antibodies may suggest a role of Daxx in 4-HNE-mediated apoptosis which would be consistent with recent studies showing that UV exposure leads to signaling for apoptosis in human 293 kidney cells via the Fas $\rightarrow$ ASK1 $\rightarrow$ Daxx $\rightarrow$ JNK pathway (*40*) because 4-HNE is generated during UV exposure and has been shown to be involved in UV-induced apoptosis (*20*). However, in the Fas $\rightarrow$ ASK1 $\rightarrow$ Daxx $\rightarrow$ JNK pathway, Daxx activates the upstream JNK kinase kinase (ASK1) leading to the activation of JNK. Our results showing the lack of ASK1 activation in 4-HNE-treated HLE B-3 cells argue against the involvement of Daxx in this process. Binding of Daxx to Fas could perhaps be attributed to its promiscuous nature of nonspecific binding with several proteins (*47*). While our studies do link the induction of Fas to JNK activation and subsequent apoptosis, our studies do not provide information about the mechanisms through which Fas-mediated signaling leads to JNK activation. Fas-mediated activation of JNK through pathways independent of FADD and Daxx has been reported (*39, 46, 48, 49*), but the exact role of upstream kinases remains undefined. Further studies are needed to elucidate role of Fas, and the intermediate steps leading to JNK activation by Fas during 4-HNE-induced apoptosis remain to be defined.

Our studies showing Fas L-independent modulation of Fas expression and its function by 4-HNE are consistent with previous studies showing ligand-independent autophospho-rylation and activation of tyrosine kinase receptor by 4-HNE (*50, 51*) These studies have shown that EGFR and PDGFR can be activated by oxidants but that their activation can be inhibited by antioxidants which scavenge ROS (*21*). How-ever, 4-HNE-induced activation of these receptors cannot be inhibited by antioxidants (*52*), indicating that 4-HNE is

the causative factor for the activation of these receptors by oxidative stress because antioxidants can inhibit oxidative stress-induced activation of these receptors by limiting 4-HNE formation but, once 4-HNE is formed, antioxidants are no longer effective. 4-HNE forms adducts with proteins (53), including cell surface proteins such as EGFR which mimic ligand−cell surface receptor binding (18). Together, these observations reaffirm the role of 4-HNE as a "small signaling molecule".

In recent years, the evidence for the involvement of 4-HNE and its metabolites in of activation of various kinases (54), expression of genes related to cell cycle events, apoptosis, etc., is mounting. The studies presented here demonstrate yet another important role of 4-HNE in the regulation of Fas which not only is an inducer of extrinsic apoptotic signaling but also has been suggested to be involved in tumorigenic pathways (6). The mechanisms through which 4-HNE regulates Fas expression are being actively pursued in our laboratory.

REFERENCES

1. Oehm, A., Behrmann, I., Falk, W., Pawlita, M., Maier, G., Klas, C., LiWeber, M., Richards, S., Dhein, J., and Trauth, B. C. (1992) Purification and molecular cloning of the APO-1 cell surface antigen, a member of the tumor necrosis factor/nerve growth factor receptor superfamily. Sequence identity with the Fas antigen, *J. Biol. Chem. 267*, 10709−10715.
2. Griffith, T. S., Brunner, T., Fletcher, S. M., Green, D. R., and Ferguson, T. A. (1995) Fas ligand-induced apoptosis as a mechanism of immune privilege, *Science 270*, 1189−1192.
3. Nagata, S. (1997) Apoptosis by death factor, *Cell 88*, 355−365.
4. Strand, S., Hofmann, W. J., Grambihler, A., Hug, H., Volkmann, M., Otto, G., Wesch, H., Mariani, S. M., Hack, V., Stremmel, W., Krammer, P. H., and Galle, P. R. (1998) Hepatic failure and liver cell damage in acute Wilson's disease involve CD95 (APO-1/Fas) mediated apoptosis, *Nat. Med. 4*, 588−593.
5. Grassme, H., Kirschnek, S., Riethmueller, J., Riehle, A., von Kurthy, G., Lang, F., Weller, M., and Gulbins, E. (2000) CD95/CD95 ligand interactions on epithelial cells in host defense to *Pseudomonas aeruginosa*, *Science 290*, 527−530.
6. O'Connell, J., O'Sullivan, G. C., Collins, J. K., and Shanahan, F. (1996) The Fas Counter attack: Fas-mediated T cell killing by colon cancer cells expressing Fas ligand, *J. Exp. Med. 184*, 1075−1082.
7. Okada, K., Komuta, K., Hashimoto, S., Matsuzaki, S., Kanematsu, T., and Koji, T. (2000) Frequency of apoptosis of tumor-infiltrating lymphocytes induced by fas counterattack in human colorectal carcinoma and its correlation with prognosis, *Clin. Cancer Res. 6*, 3560−3564.
8. Peter, M. E., Heufelder, A. E., and Hengartner, M. O. (1997) Advances in apoptosis research, *Proc. Natl. Acad. Sci. U.S.A. 94*, 12736−12737.
9. Chiarpotto, E., Domenicotti, C., Paola, D., Vitali, A., Nitti, M., Pronzato, M. A., Biasi, F., Cottalasso, D., Marinari, M. U., Dragonetti, A., Cesaro, P., Isodoro, C., and Poli, G. (1999) Regulation of rat hepatocyte protein kinase Cβ isoenzymes by the lipid peroxidation product 4-hydroxy-2,3-nonenal: A signaling pathway to modulate vesicular transport of glycoproteins, *Hepatology 29*, 1565−1572.
10. Esterbauer, H., Schaur, R. J., and Zollner, H. (1991) Chemistry and biochemistry of 4-hydroxynonenal, malonaldehyde and related aldehydes, *Free Radical Biol. Med. 23*, 81−128.
11. Fazio, V. M., Barrera, G., Martinotti, S., Farace, M. G., Giglioni, B., Frati, L., Manzari, V., and Dianzani, M. U. (1992) 4-Hydroxynonenal, a product of cellular lipid peroxidation, which modulates c-myc and globin gene expression in K562 erythroleukemic cells, *Cancer Res. 52*, 4866−4871.
12. Parola, M., Robino, G., Marra, F., Pinzano, M., Bellomo, G., Leonarduzzi, G., Chiarugi, P., Camandola, S., Poli, G., Waeg, G., Gentilini, P., and Dianzani, M. U. (1998) HNE interacts directly with JNK isoforms in human hepatic stellate cells, *J. Clin. Invest. 102*, 1942−1950.
13. Cheng, J. Z., Singhal, S. S., Saini, M. K., Singhal, J., Piper, J. T., Van Kuijk, F. T., Zimniak, P., Awasthi, Y. C., and Awasthi, S. (1999) Effects of mGST A4 transfection on 4-hydroxynonenal-mediated apoptosis and differentiation of K562 human erythroleukemia cells, *Arch. Biochem. Biophys. 372*, 29−36.
14. Uchida, K., Shiraishi, M., Naito, Y., Torii, Y., Nakamura, Y., and Osawa, T. (1999) Activation of stress signaling pathways by the end product of lipid peroxidation. 4-Hydroxy-2-nonenal is a potential inducer of intracellular peroxide production, *J. Biol. Chem. 274*, 2234−2242.
15. Yang, Y., Cheng, J. Z., Singhal, S. S., Saini, M., Pandya, U., Awasthi, S., and Awasthi, Y. C. (2001) Role of glutathione S-transferases in protection against lipid peroxidation. Overexpression of hGSTA2-2 in K562 cells protects against hydrogen peroxide-induced apoptosis and inhibits JNK and caspase 3 activation, *J. Biol. Chem. 276*, 19220−19230.
16. Cheng, J. Z., Sharma, R., Yang, Y., Singhal, S. S., Sharma, A., Saini, M. K., Singh, S. V., Zimniak, P., Awasthi, S., and Awasthi, Y. C. (2001) Accelerated metabolism and exclusion of 4-hydroxynonenal through induction of RLIP76 and hGST5.8 is an early adaptive response of cells to heat and oxidative stress, *J. Biol. Chem. 276*, 41213−41223.
17. Dickinson, D. A., Iles, K. E., Watanabe, N., Iwamoto, T., Zhang, H., Karzywanski, D. M., and Foreman, H. J. (2002) 4-Hydroxynonenal induces glutamate cysteine ligase through JNK in HBE1 cells, *Free Radical Biol. Med. 33*, 974−987.
18. Nakashima, I., Liu, W., Akhand, A. A., Takeda, K., Kawamoto, Y., Kato, M., and Suzuki, H. (2003) 4-Hydroxynonenal triggers multistep signal transduction cascades for suppression of cellular functions, *Mol. Aspects Med. 24*, 231−238.
19. Dianzani, M. U. (2003) 4-Hydroxynonenal from pathology to physiology, *Mol. Aspects Med. 24*, 263−272.
20. Yang, Y., Sharma, A., Sharma, R., Patrick, B., Singhal, S. S., Zimniak, P., Awasthi, S., and Awasthi, Y. C. (2003) Cells preconditioned with mild, transient UVA irradiation acquire resistance to oxidative stress and UVA-induced apoptosis: Role of 4-hydroxynonenal in UVA-mediated signaling for apoptosis, *J. Biol. Chem. 278*, 41380−41388.
21. Negre-Salvayre, A., Vieira, O., Escarguil-Blane, I., and Salvayre, R. (2003) Oxidized LDL and 4-hydroxynonenal modulate tyrosine kinase receptor activity, *Mol. Aspects Med. 24*, 251−261.
22. Awasthi, Y. C., Yang, Y., Tiwari, N. K., Patrick, B., Sharma, A., Li, J., and Awasthi, S. (2004) Regulation of 4-hydroxynonenal-mediated signaling by glutathione S-transferases, *Free Radical Biol. Med. 37*, 607−619.
23. Barrera, G., Pizzimenti, S., and Dianzani, M. U. (2004) 4-Hydroxynonenal and regulation of cell cycle: Effects on the pRb/E2F pathway, *Free Radical Biol. Med. 37*, 597−606.
24. Forman, H. J., and Dickinson, D. A. (2004) Introduction to serial reviews on 4-hydroxy-2-nonenal as a signaling molecule, *Free Radical Biol. Med. 37*, 594−596.
25. Petersen, D. R., and Doorn, J. A. (2004) Reactions of 4-hydroxynonenal with proteins and cellular targets, *Free Radical Biol. Med. 37*, 937−945.
26. Leonarduzzi, G., Robbesyn, F., and Poli, G. (2004) Signaling kinases modulated by 4-hydroxynonenal, *Free Radical Biol. Med. 37*, 1694−1702.
27. Marinari, U. M., Nitti, M., Pronzato, M. A., and Domenicotti, C. (2003) Role of PKC-dependent pathways in HNE-induced cell protein transport and secretion, *Mol. Aspects Med. 24*, 205−211.
28. Patrick, B., Li, J., Jeyabal, P. V., Reddy, P. M., Yang, Y., Sharma, R., Sinha, M., Luxon, B., Zimniak, P., Awasthi, S., and Awasthi, Y. C. (2005) Depletion of 4-hydroxynonenal in hGSTA4-transfected HLE B-3 cells results in profound changes in gene expression, *Biochem. Biophys. Res. Commun. 334*, 425−432.
29. Sharma, R., Brown, D., Awasthi, S., Yang, Y., Sharma, A., Patrick, B., Saini, M. K., Singh, S. P., Zimniak, P., Singh, S. V., and Awasthi, Y. C. (2004) Transfection with 4-hydroxynonenal-metabolizing glutathione S-transferase isozymes leads to phenotypic transformation and immortalization of adherent cells, *Eur. J. Biochem. 271*, 1690−1701.
30. Sharma, R., Yang, Y., Sharma, A., Dwivedi, S., Popov, V. L., Boor, P. J., Singhal, S. S., Awasthi, S., and Awasthi, Y. C. (2003) Mechanisms and physiological significance of the transport of the glutathione conjugate of 4-hydroxynonenal in human lens epithelial cells, *Invest. Ophthalmol. Visual Sci. 44*, 3438−3449.

31. Kruman, I., Bruce-Keller, A. J., Bredesen, D., Waeg, G., and Mattson, M. P. (1997) Evidence that 4-hydroxynonenal mediates oxidative stress-induced neuronal apoptosis, *J. Neurosci. 17*, 5089−5100.

32. Awasthi, Y. C., Sharma, R., Cheng, J. Z., Yang, Y., Sharma, A., Singhal, S. S., and Awasthi, S. (2003) Role of 4-hydroxynonenal in stress-mediated apoptosis signaling, *Mol. Aspects Med. 24*, 219−230.

33. Engle, M. R., Singh, S. P., Czernik, P. J., Gaddy, D., Montague, D. C., Ceci, J. D., Yang, Y., Awasthi, S., Awasthi, Y. C., and Zimniak, P. (2004) Physiological role of mGSTA4-4, a glutathione S-transferase metabolizing 4-hydroxynonenal: Generation and analysis of mGsta4 null mouse, *Toxicol. Appl. Pharmacol. 194*, 296−308.

34. Cheng, J. Z., Yang, Y., Singh, S. P., Singhal, S. S., Awasthi, S., Pan, S. S., Singh, S. V., Zimniak, P., and Awasthi, Y. C. (2001) Two distinct 4-hydroxynonenal metabolizing glutathione S-transferase isozymes are differentially expressed in human tissues, *Biochem. Biophys. Res. Commun. 282*, 1268−1274.

35. Hartley, D. P., Ruth, J. A., and Petersen, D. R. (1995) The hepatocellular metabolism of 4-hydroxynonenal by alcohol dehydrogenase, aldehyde dehydrogenase, and glutathione S-transferase, *Arch. Biochem. Biophys. 316*, 197−205.

36. Bradford, M. M. (1976) A rapid and sensitive method for the quantitation of microgram quantities of protein utilizing the principle of protein-dye binding, *Anal. Biochem. 72*, 248−254.

37. Peter, M. E., Legembre, P., and Barnhart, B. C. (2005) Does CD95 have tumor promoting activities? *Biochim. Biophys. Acta 1755*, 25−36.

38. Chang, H. Y., Nishitoh, H., Yang, X., Ichijo, H., and Baltimore, D. (1998) Activation of apoptosis signal-regulating kinase 1 (ASK1) by the adapter protein Daxx, *Science 281*, 1860−1863.

39. Yang, X., Khosravi-Far, R., Chang, H. Y., and Baltimore, D. (1997) Daxx, a novel Fas-binding protein that activates JNK and apoptosis, *Cell 87*, 1067−1076.

40. Wu, S., Loke, H. N., and Rehemtulla, A. (2002) Ultraviolet radiation-induced apoptosis is mediated by Daxx, *Neoplasia 4*, 486−492.

41. Paradisi, L., Panagini, C., Parola, M., Barrera, G., and Dianzani, M. U. (1985) Effects of 4-hydroxynonenal on adenylate cyclase and 5′-nucleotidase activities in rat liver plasma membranes, *Chem.-Biol. Interact. 53*, 209−217.

42. Rossi, M. A., Fidale, F., Garramone, A., Esterbauer, H., and Dianzani, M. U. (1990) Effect of 4-hydroxylalkenals on hepatic phosphatidylinositol-4,5-bisphosphate-phospholipase C, *Biochem. Pharmacol. 39*, 1715−1719.

43. Rinaldi, M., Barrera, G., Aquino, A., Spinsanti, P., Pizzimenti, S., Farace, M. G., Dianzani, M. U., and Fazio, V. M. (2000) 4-Hydroxynonenal-induced MEL cell differentiation involves PKC activity translocation, *Biochem. Biophys. Res. Commun. 272*, 75−80.

44. Engle, M. R., Singh, S. P., Czernik, P., Shammas, M. A., Ceci, J. D., Yang, Y., Awasthi, S., Zimniak, L., and Zimniak, P. (2004) *mGSTA4* null mouse: Generation and characterization, Second meeting of the HNE-Club: HNE and Lipid Peroxidation Products: From Basic Science to Medicine, Berlin, July 6−9.

45. Desbarats, J., and Newell, M. K. (2000) Fas engagement accelerates liver regeneration after partial hepatectomy, *Nat. Med. 6*, 920−923.

46. Salomoni, P., and Khelifi, A. F. (2006) Daxx: Death or survival protein? *Trends Cell Biol. 16*, 97−104.

47. Michaelson, J. S., Bader, D., Kuo, F., Kozak, C., and Leder, P. (1999) Loss of Daxx, a promiscuously interacting protein, results in extensive apoptosis in early mouse development, *Genes Dev. 13*, 1918−1923.

48. Goillot, E., Raingeaud, J., Ranger, A., Tepper, R. I., Davis, R. J., Harlow, E., and Sanchez, I. (1997) Mitogen-activated protein kinase-mediated Fas apoptotic signaling pathway, *Proc. Natl. Acad. Sci. U.S.A. 94*, 3302−3307.

49. Latinis, K. M., and Koretzky, G. A. (1996) Fas ligation induces apoptosis and Jun kinase activation independently of CD45 and Lck in human T cells, *Blood 87*, 871−875.

50. Heldin, C. H., Ostman, A., and Ronnstrand, L. (1998) Signal transduction via platelet-derived growth factor receptors, *Biochim. Biophys. Acta 1378*, 79−113.

51. Escargueil-Blanc, I., Salvayre, R., Vacaresse, N., Jurgens, G., Darblade, B., Arnal, J. F., Parthasarathy, S., and Negre-Salvayre, A. (2001) Mildly oxidized LDL induces activation of platelet-derived growth factor β-receptor pathway, *Circulation 104*, 1814−1821.

52. Vacaresse, N., Vieira, O., Robbesyn, F., Jurgens, G., Salvayre, R., and Negre-Salvayre, A. (2001) Phenolic antioxidants trolox and caffeic acid modulate the oxidized LDL-induced EGF-receptor activation, *Br. J. Pharmacol. 132*, 1777−1788.

53. Uchida, K., Szweda, L. I., Chae, H. Z., and Stadtman, E. R. (1993) Immunochemical detection of 4-hydroxynonenal protein adducts in oxidized hepatocytes, *Proc. Natl. Acad. Sci. U.S.A. 90*, 8742−8746.

54. Srivastava, S. K., Ramana, K. V., and Bhatnagar, A. (2005) Role of aldose reductase and oxidative damage in diabetes and the consequent potential for therapeutic options, *Endocr. Rev. 26*, 380−392.